DNA Bending and Binding by Metallo-Zipper Models of bZIP Proteins

C. Rodgers Palmer,[‡] Leslie S. Sloan,[§] James C. Adrian, Jr.,[§,†] Bernard Cuenoud,[§,⊥] David N. Paolella,[§,||] and Alanna Schepartz*[,§,||]

Contribution from the Department of Chemistry, Department of Molecular Biophysics and Biochemistry, and Training Program in Biophysics, Yale University, New Haven, Connecticut 06520

Received April 13, 1995[⊗]

Abstract: The metallo-peptide $[G_{29}T_S]_2Fe$ contains two copies of the DNA recognition peptide of the yeast bZIP protein GCN4 assembled into a dimer with a 4′-substituted bis(terpyridyl)iron(II) complex. $[G_{29}T_S]_2Fe$ contains the same DNA recognition peptide as GCN4, yet it possesses a function that GCN4 does not: it discriminates between the CRE (ATGACGTCAT) and AP-1 (ATGACTCAT) target sites, two bZIP target sites that differ by the presence or the absence of a single G·C base pair. In terms of its CRE/AP-1 specificity, $[G_{29}T_S]_2Fe$ resembles the bZIP proteins CREB and CRE-BP1, whose biological functions require accurate discrimination of these two target sites. Here are described a series of experiments that explore the molecular basis for the high CRE/AP-1 specificity of $[G_{29}T_S]_2Fe$ and its homologue $[G_{28}T_S]_2Fe$. Quantitative analysis of equilibrium dissociation constants reveals that the stabilities of the $[G_{28}T_S]_2Fe$·CRE and $[G_{29}T_S]_2Fe$·CRE complexes are no higher than those of the corresponding disulfide-dimer·CRE complexes. In addition, the phosphate interference patterns of the $[G_{28}T_S]_2Fe$·CRE and $[G_{29}T_S]_2Fe$·CRE complexes superpose on those of the corresponding disulfide-dimer·CRE complexes. Finally, helical phasing analysis reveals that the metallo-peptides and the disulfide-dimer peptides all induce equivalent distortions in the DNA. However, CRE/AP-1 specificity is eliminated when the bis(terpyridyl)iron(II) complex is replaced by a sterically less-demanding bipyridyl moiety. This result, analyzed in the context of recently solved structures of GCN4 bound to the CRE and AP-1 target sites, leads us to propose that CRE/AP-1 specificity results from interactions between the bis(terpyridyl)iron(II) complex and the proximal region of the peptide that disrupts one or more critical protein·AP-1 interactions. Remarkably, the mechanism of CRE/AP-1 specificity proposed for the metallo-peptide bZIP models mirrors, at least in part, the mechanism employed by the naturally CRE-selective proteins CREB and CRE-BP1. Our observation that subtle and indirect effects on the conformation of a short peptide can lead to large changes in DNA target specificity provides evidence that it may be possible to design surprisingly small molecules that bind DNA with high sequence-specificity as well as high affinity.

Introduction

Transition-metal complexes provide a convenient and adaptable scaffold for the assembly of functional synthetic arrays.[1-10] In our laboratory, we have exploited transition-metal complexes as scaffolds for the assembly of synthetic receptors that possess a measurable function.[1] This idea took form initially in 1989 with the synthesis of bis(salicylaldimine)nickel(II) complexes that assembled flexible polyether chains into ionophores capable of selectively transporting cations across a synthetic membrane.[1,9] More recently we exploited the high stabilities and defined geometries of bis(terpyridyl)iron(II) complexes[12] to organize peptides into complexes that bound DNA with specificities that depended on the precise structure of the metal complex.[13-15]

The complexes we prepared contained two copies of the DNA recognition peptide of the yeast transcriptional activator GCN4[16-20] assembled into a dimer with one of three differentially substituted bis(terpyridyl)iron(II) complexes.[13-15] One of these complexes, $[G_{29}T_S]_2Fe$ (Figure 1A) was exceptionally interesting because it possessed a function that GCN4 itself did not: it discriminated between the CRE (ATGACGTCAT) and AP-1 (ATGACTCAT) target sites, two bZIP target sites that

* To whom correspondence should be addressed.
† Current address: Department of Chemistry, Union College.
‡ Department of Molecular Biophysics and Biochemistry.
§ Department of Chemistry.
⊥ Current address: Ciba-Geigy Ltd., Basel, Switzerland.
|| Training Program in Biophysics.
⊗ Abstract published in *Advance ACS Abstracts,* August 15, 1995.

(1) Schepartz, A.; McDevitt, J. P. *J. Am. Chem. Soc.* **1989**, *111*, 5976.
(2) Sasaki, T.; Kaiser, T. *J. Am. Chem. Soc.* **1989**, *111*, 380.
(3) Pyle, A. M.; Barton, J. K. *Prog. Inorg. Chem.* **1990**, *38*, 413 and references cited therein.
(4) Lieberman, M.; Sasaki, T. *J. Am. Chem. Soc.* **1991**, *113*, 1470.
(5) Schwabacher, A. W.; Lee, J.; Lei, H. *J. Am. Chem. Soc.* **1992**, *114*, 7597.
(6) Ghadiri, M. R.; Soares, C.; Choi, C. *J. Am. Chem. Soc.* **1992**, *114*, 825.
(7) Fujimoto, K.; Shinkai, S. *Tetrahedron Lett.* **1994**, *35*, 2915.
(8) Goodman, M. S.; Weiss, J.; Hamilton, A. D. *Tetrahedron Lett.* **1994**, *35*, 8943.
(9) Jones, M. W.; Gupta, N.; Schepartz, A.; Thorp, H. H. *Inorg. Chem.* **1992**, *31*, 1308.
(10) For examples of nonmetallic scaffolds for the assembly of functional synthetic arrays, see: Ueno, M.; Murakami, A.; Makino, K.; Morii, T. *J. Am. Chem. Soc.* **1993**, *115*, 12575; Morii, R.; Simomura, M.; Morimoto, S.; Saito, I. *J. Am. Chem. Soc.* **1993**, *115*, 1150, as well as ref 11.
(11) Schall, O. F.; Gokel, G. W. *J. Am. Chem. Soc.* **1994**, *116*, 6089.
(12) Morgan, G. T.; Burstall, F. H. *J. Chem. Soc.* **1932**, *135*, 20.
(13) Cuenoud, B.; Schepartz, A. *Tetrahedron Lett.* **1991**, *32*, 3325.
(14) Cuenoud, B.; Schepartz, A. *Science* **1993**, *259*, 510.
(15) Cuenoud, B.; Schepartz, A. *Proc. Natl. Acad. Sci. U.S.A.* **1993**, *90*, 1154.
(16) Penn, M. D.; Galgoci, B.; Greer, H. *Proc. Natl. Acad. Sci. U.S.A.* **1983**, *80*, 2704.
(17) Hinnebusch, A. G.; Fink, G. R. *Proc. Natl. Acad. Sci. U.S.A.* **1983**, *80*, 5374.
(18) Ellenberger, T. E.; Brandl, C. J.; Struhl, K.; Harrison, S. C. *Cell* **1992**, *71*, 1223.
(19) König, P.; Richmond, T. *J. Mol. Biol.* **1993**, *233*, 139.
(20) For a review of bZIP proteins, see: Hurst, H. C. *Protein Profile* **1994**, *1*, 123.

0002-7863/95/1517-8899$09.00/0

differed by the presence or the absence of a single G·C base pair. GCN4 formed roughly iso-energetic complexes with these two target sites.[21,22] $[G_{29}T_S]_2Fe$, in contrast, displayed high selectivity for the CRE target site: it bound the CRE target site with an apparent binding energy ($\Delta G°_{obs}$) 2−4 kcal·mol^{-1} greater than that with which it bound the AP-1 target site, depending on reaction conditions.[15] Little or no CRE/AP-1 specificity (<1 kcal·mol^{-1}) was observed when the two G_{29} peptides were joined by a Gly-Gly-Cys disulfide linker.[13-15] By use of competition experiments, we showed that the high target-site specificity exhibited by $[G_{29}T_S]_2Fe$ resulted from a selection against the AP-1 target site as opposed to a selection for the CRE target site.[15] The remarkable level of CRE/AP-1 specificity exhibited by $[G_{29}T_S]_2Fe$ exceeded that of natural bZIP proteins in the CREB/ATF family whose biological functions require them to discriminate between the CRE and AP-1 target sites.[22,23]

The CRE and AP-1 target sites recognized by GCN4 differ only by the presence or absence of a single base pair located between two ATGA half sites. Were both target sites to assume canonical B DNA conformations, then the additional base pair in the center of the CRE target site would displace each ATGA half site from the position it occupied in the AP-1 target site by an axial translation of 3.25 Å and a twist angle of 34.5°. This geometric operation corresponds to a 4 Å displacement of each base and a 7 Å displacement of each phosphate.[19] This change represents a substantial structural perturbation, and therefore it should not be surprising that certain bZIP proteins as well as certain bis(terpyridyl-peptide)iron(II) complexes, prefer one site to the other. However, recent results from our laboratory indicate that the CRE target site does not assume a canonical B DNA conformation, rather, it bends intrinsically toward the major groove by 10−15 degrees.[24] This result, in conjunction with the recently reported crystal structures of the GCN4 bZIP·CRE[19] and GCN4 bZIP·AP-1[18] complexes, led us to propose that the intrinsic bend in the CRE target site compensates structurally for the extra base pair in its sequence and equates its recognition interface to that of the AP-1 target site.[24] The proposal that the CRE and AP-1 bZIP target sites are equated by an intrinsic bend accounts for the otherwise unexplained ability of GCN4 to form energetically similar complexes with them.[21,22,24]

But if the recognition interfaces of the CRE and AP-1 target sites are equated so that GCN4 recognizes both, then how does $[G_{29}T_S]_2Fe$ select against the AP-1 target site? Here we describe a series of experiments designed to reveal how bis(terpyridyl)-iron(II) complexes derived from GCN4 discriminate between the CRE and AP-1 target sites. Several different bis(terpyridyl)-iron(II) complexes were analyzed to determine their target site selectivities and sensitivity to phosphate ethylation as well as their effects on the conformations of the CRE and AP-1 target sites. Parallel experiments were performed with the corresponding disulfide-dimer peptides,[25,26] which showed no CRE/AP-1 selectivity.[14] Our initial results revealed that despite the differences in their target-site selectivities, the bis(terpyridyl)-iron(II) complexes and the corresponding disulfide-dimer peptides formed complexes with the CRE target site that were virtually indistinguishable in terms of their equilibrium dissociation constants, sensitivity to phosphate ethylation, and extent of peptide-induced DNA distortion. The bis(terpyridyl)-iron(II) complex may alter CRE/AP-1 specificity, but it does not alter detectably the interactions between the G_{28} and G_{29} peptides and the CRE target site.

We then focused our attention on the bis(terpyridyl)iron(II) complex itself. In particular, we wondered whether specificity resulted from interactions between the bulky bis(terpyridyl)-iron(II) complex and either the DNA or the attached peptide, that destabilized selectively the peptide·AP-1 complex. To test this idea, we synthesized a molecule containing a bipyridine moiety in place of the bis(terpyridyl)iron(II) complex. The rigid bipyridine moiety separated the C-termini of the GCN4 DNA recognition peptides by approximately the same distance as did the bis(terpyridyl)iron(II) complex but was far less demanding sterically (*vide infra*). The bipyridine-linked peptide dimer behaved much like a disulfide-dimer peptide and bound the CRE and AP-1 target sites with comparable affinity. This result, analyzed in the context of recently solved structures of GCN4 bound to the CRE and AP-1 target sites,[18,19] leads us to propose that the high CRE/AP-1 specificity of the metallo-peptides results from interactions between the bis(terpyridyl)iron(II) complex and the proximal region of the peptide, the "spacer segment", that disrupts one or more critical protein·AP-1 interactions. Remarkably, the mechanism of CRE/AP-1 specificity proposed for the metallo-peptide models mirrors, at least in part, the mechanism employed by the naturally CRE-selective proteins CREB and CRE-BP1.[22]

Results

Synthesis and Analysis of $[G_{28}T_S]_2Fe$. First we ruled out the possibility that the selectivity of $[G_{29}T_S]_2Fe$ was an artifact related to the presence of the non-native Gly-Gly linker at the carboxyl terminus or to the non-native serine residue at the amino terminus of the G_{29} peptide. We synthesized a new peptide, G_{28}, which differed from the G_{29} peptide by the absence of two C-terminal glycine residues as well as by two changes at the amino terminus that regenerated the native GCN4 sequence (Figure 1A). The bis(terpyridyl)iron(II) complex containing G_{28}, $[G_{28}T_S]_2Fe$, and the corresponding disulfide-dimer peptide G_{28}^{SS} were synthesized and purified as described previously for $[G_{29}T_S]_2Fe$ and G_{29}^{SS}.[13-15] Qualitative electrophoretic mobility shift analyses (EMSA)[27,28] demonstrated that $[G_{28}T_S]_2Fe$, like $[G_{29}T_S]_2Fe$, bound avidly to a DNA probe containing the CRE target site but poorly to a probe containing the AP-1 target site (Figure 2A). The equilibrium dissociation constant of the $[G_{28}T_S]_2Fe$·CRE complex was approximately 1 nM; the dissociation constant of the $[G_{28}T_S]_2Fe$·AP-1 complex was greater than that of a complex with nonspecific DNA. As expected, the disulfide-dimer peptide G_{28}^{SS} bound well to both sites with dissociation constants of about 4 nM (Figure 2A).

The relative DNA affinities of the metallo-zipper and disulfide-dimer peptides were determined more precisely by use of a competition electrophoretic mobility shift assay.[15] Each peptide was incubated with a 5′-end labeled 24 bp oligonucleotide probe containing a central CRE target site (CRE_{24}) in the presence of varying concentrations of an unlabeled specific (CRE, AP-1) or nonspecific (SCR, C30) oligonucleotide. Plots showing the fraction of end-labeled CRE_{24} bound to the indicated peptide at equilibrium as a function of the competitor DNA concentration are shown in Figure 2B. In each case, the data fit a theoretical equation describing the two linked equilibria.[15] Equilibrium dissociation constants of the 16 DNA·peptide complexes calculated from these plots are pre-

(21) Sellers, J. W.; Vincent, A. C.; Struhl, K. *Mol. Cell. Biol.* **1990**, *10*, 5077.
(22) Metallo, S. J.; Schepartz, A. *Chemistry Biology* **1994**, *1*, 143.
(23) Habener, J. F. *Mol. Endocrin.* **1990**, *4*, 1087.
(24) Paolella, D. N.; Palmer, C. R.; Schepartz, A. *Science* **1994**, *264*, 1130.
(25) Talanian, R. V.; McKnight, C. J.; Kim, P. S. *Science* **1990**, *249*, 769.
(26) Talanian, R. V.; McKnight, C J.; Rutkowski, R.; Kim, P. S. *Biochemistry* **1992**, *31*, 6871.
(27) Fried, M.; Crothers, D. M. *Nuc. Acids Res.* **1981**, *9*, 6505.
(28) Garner, M. M.; Revzin, A. *Nuc. Acids Res.* **1981**, *9*, 3047.

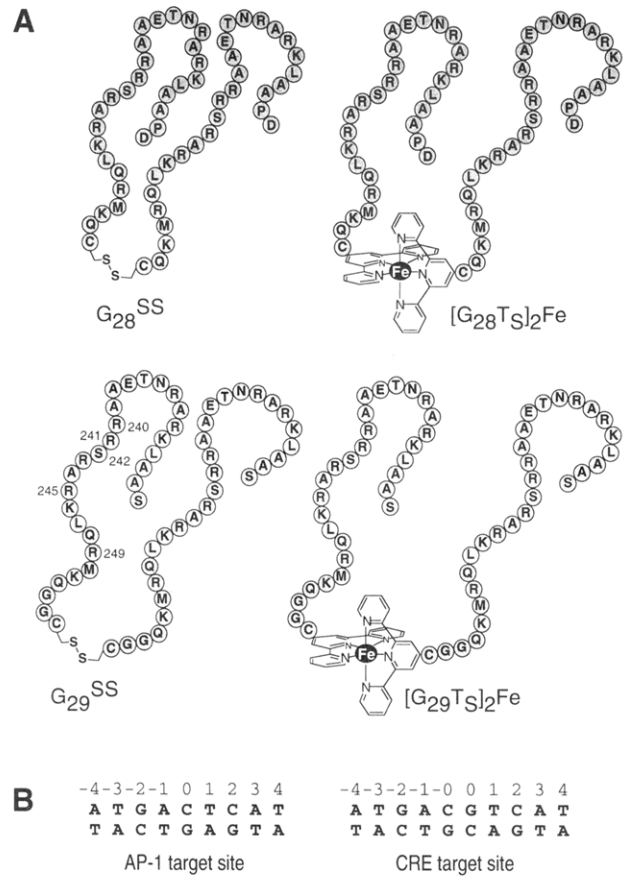

Figure 1. (A) Metallo-zipper[13-15] and disulfide-dimer peptides[25,26] used in this study. GCN4 residues discussed in the text are identified on the corresponding position of G_{29}^{SS}. (B) The consensus AP-1 and CRE target sites of bZIP proteins.

sented in Table 1. In this study, conditions of pH, buffer, and salt concentration were chosen to minimize nonspecific DNA interactions; in particular, the salt concentration was higher than that used previously.[14,15]

All four peptides bound the CRE target site with dissociation constants of approximately 1 nM, but their affinities for the AP-1 target site varied over a broad range. The two disulfide-dimer peptides bound the AP-1 target site considerably better than they bound the "nonspecific" DNA sequences SCR and C30, while the two metallo-zipper peptides bound the AP-1 sequence considerably more poorly than they bound the "nonspecific" DNA sequences. In terms of their CRE/AP-1 specificities, $[G_{28}T_S]_2Fe$ and $[G_{29}T_S]_2Fe$ were 2.3 and 1.3 kcal·mol^{-1} more CRE-selective than were the corresponding disulfide-dimer peptides. In addition, $[G_{28}T_S]_2Fe$ was about 0.5 kcal·mol^{-1} more CRE-selective than was $[G_{29}T_S]_2Fe$. The increase in specificity was due to a slightly increased CRE affinity and a slightly decreased AP-1 affinity: $[G_{28}T_S]_2Fe$ bound the CRE target site with 0.3 kcal mol^{-1} greater affinity and the AP-1 target site with 0.2 kcal mol^{-1} lower affinity than did $[G_{29}T_S]_2Fe$. These experiments confirmed that the high CRE specificity observed with $[G_{29}T_S]_2Fe$ was not an artifact attributable to the non-native Gly-Gly linker or to the amino terminal serine residue.

Interference Assays. Phosphate ethylation interference assays were performed on the CRE complexes of $[G_{28}T_S]_2Fe$, $[G_{29}T_S]_2Fe$, G_{28}^{SS}, and G_{29}^{SS} to determine if there were major differences in the peptide·phosphate contacts within each complex. Naked DNA was treated with ethylnitrosourea to alkylate unesterified phosphate oxygen atoms, and the partially modified DNA was incubated with peptide at a concentration approximating the equilibrium dissociation constant.[29,30] Free and peptide bound DNA molecules were resolved by nondenaturing gel electrophoresis, eluted from the gel, cleaved with

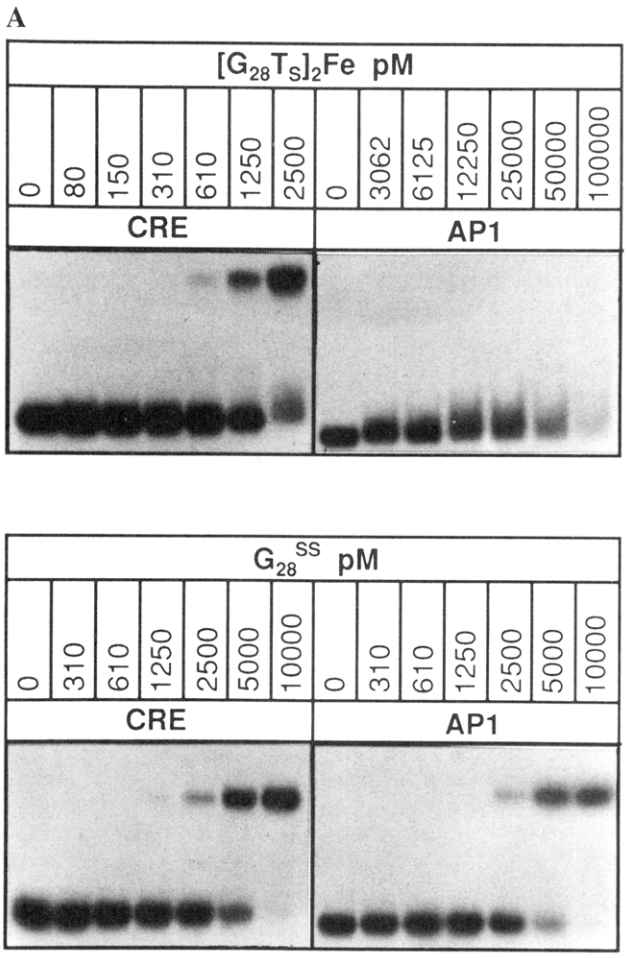

Figure 2. (A) Autoradiograms illustrating electrophoretic mobility shift analysis of the CRE_{24} and AP-1_{23} complexes of $[G_{28}T_S]_2Fe$ and G_{28}^{SS}. (B) Electrophoretic mobility shift competition analysis of the relative affinities of $[G_{29}T_S]_2Fe$, $[G_{28}T_S]_2Fe$, G_{29}^{SS}, and G_{28}^{SS} for specific and nonspecific DNAs. Semilogarithmic plots illustrate the fraction ^{32}P CRE_{24} (Θ) bound to peptide as a function of added competitor DNA. Error bars shown for competition by CRE (○), AP-1 (□), C30 (▲), and SCR (♦) represent the standard deviation of at least three independent experiments. Solid lines represent the best fit of the data to eq 2.

(29) Johnson-Liu, H.-N.; Gartenberg, M. R.; Crothers, D. M. *Cell* **1986**, *47*, 995.

(30) Gartenberg, M. R.; Ampe, C.; Steitz, T. A.; Crothers, D. M. *Proc. Natl. Acad. Sci. U.S.A.* **1990**, *87*, 6034.

Table 1. Equilibrium Dissociation Constants at 4 °C of Peptide•DNA Complexes Determined by Competition Analysis[a]

peptide	K_d (nM) [$\Delta G°_{obs}$ (kcal•mol^{-1})]				$\Delta\Delta G°_{obs}$ (kcal•mol^{-1})	
	CRE[c]	AP-1	SCR	C30	CRE/AP-1[d]	CRE/NSP[e]
G_{28}^{SS}	0.25 ± 0.03 [−12.2]	1.45 ± 0.24 [−11.2]	150 ± 43 [−8.7]	152 ± 54 [−8.6]	−1.0	−3.6
G_{29}^{SS}	0.96 ± 0.19 [−11.4]	14.5 ± 1.4 [−9.9]	92.3 ± 11.4 [−8.9]	58.8 ± 19.2 [−9.2]	−1.5	−2.3
$[G_{28}T_S]_2Fe$	0.66 ± 0.10 [−11.6]	292 ± 85 [−8.3]	129 ± 25 [−8.7]	82.9 ± 41 [−9.0]	−3.3	−2.8
$[G_{29}T_S]_2Fe$	1.29 ± 0.35 [−11.3]	182 ± 28 [−8.5]	81.1 ± 19 [−9.0]	26.0 ± 11 [−9.6]	−2.8	−2.0

[a] Details are found in the Experimental Section. Binding buffer: 10 mM potassium phosphate pH 7.4, 100 mM KCl, 0.1% Nonidet P-40, 5% glycerol. [b] Calculated from the relationship $\Delta G°_{obs} = -RT \ln (1/K_d)$ where $R = 0.001\,987$ kcal•mol^{-1}•K^{-1} and $T = 277$ K. [c] **CRE$_{24}$**, d(AGTGGAGATGACGTCATCTCGTGC); **AP-1$_{23}$**, d(AGTGGAGATGACTCATCTCGTGC); **C$_{30}$**, d(GATATCCCTGTTACGACTTGAGGATCAAAG); **SCR**, d(AGTGGAGTAAGGCCTATCTCGTGC). [d] Calculated from the relationship $\Delta\Delta G°_{obs} = \Delta G°_{obs}(CRE) - \Delta G°_{obs}(AP\text{-}1)$. [e] Calculated from the relationship $\Delta\Delta G°_{obs} = \Delta G°_{obs}(CRE) - \Delta G°_{obs}(NSP)$ where $\Delta G°_{obs}(NSP)$ is the average of $\Delta G°_{obs}(SCR)$ and $\Delta G°_{obs}(C30)$ and NSP = nonspecific DNA.

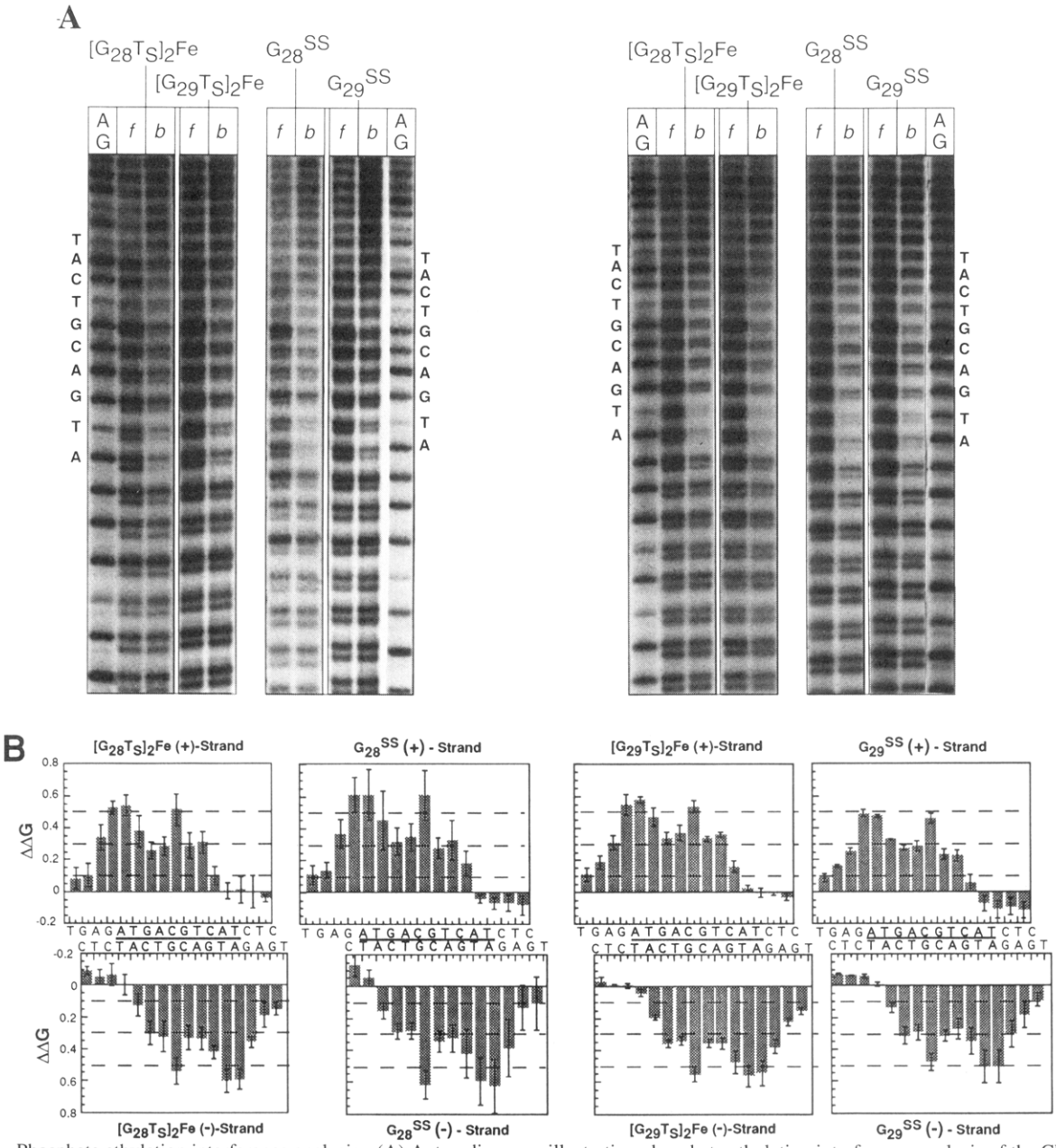

Figure 3. Phosphate ethylation interference analysis. (A) Autoradiograms illustrating phosphate ethylation interference analysis of the CRE target site in the presence of G_{29}^{SS}, G_{28}^{SS}, $[G_{28}T_S]_2Fe$, and $[G_{29}T_S]_2Fe$. The region corresponding to the 10 bp CRE target site is indicated alongside A+G sequencing lanes labeled AG; f and b correspond to the free (protein unbound) and bound (protein bound) fractions obtained after native gel electrophoresis (see Experimental Section for details). DNA that is alkylated on a phosphate oxygen cleaves under alkaline conditions to produce products with 3′-OH termini (which comigrate with the corresponding products of acid hydrolysis in the A+G lanes) and 3′-phosphate termini (which migrate slightly faster than the products of acid hydrolysis). The panel on the left shows the analysis of the top (+) strand; the panel on the right, the bottom (−) strand. (B) Plots of the reduction in relative Gibbs free energy of binding (in kcal•mol^{-1}) as a function of the position of phosphate ethylation. The consensus CRE target site is underlined. Error bars represent the standard deviation of at least three experiments.

alkali, and separated on a high resolution sequencing gel. A sample of the primary data is shown in Figure 3A. Histograms illustrating the loss in binding free energy that occurred upon ethylation of each individual phosphate are shown in Figure

3B. We did not determine the ethylation intereference patterns of the corresponding AP-1 complexes since we were unable to observe the AP-1 complexes of the two metallo-peptides under these conditions.

All four peptide•CRE complexes were sensitive to phosphate ethylation at 9−12 consecutive positions on each DNA strand. In each case, the effects of phosphate ethylation on binding affinity were disposed symmetrically about the dyad axis of the CRE target site and shifted to the 5′ side, consistent with a model in which the peptide interacts with DNA in the major groove.[31,32] Maximal interference was observed at phosphates $G_{-5}pA_{-4}$, $A_{-4}pT_{-3}$, $T_{-3}pG_{-2}$, and $C_{-0}pG_0$, with smaller effects at phosphates $G_{-2}pA_{-1}$, $A_{-1}pC_{-0}$, G_0pT_1, T_1pC_2, and C_2pA_3 (see Figure 1 for numbering scheme). The positions of maximal interference corresponded to phosphates that participate in direct protein contacts in the X-ray structure of GCN4 bound to the CRE target site.[19] Ethylation at the $G_{-5}pA_{-4}$ step blocked the paired salt-bridge and H-bond contacts of Arg_{241} and Arg_{245}, respectively; ethylation at the $A_{-4}pT_{-3}$ step blocked the paired H-bond contacts from Arg_{245} and Ser_{242}; ethylation at the central $C_{-0}pG_0$ step blocked a single H-bond donated by Arg_{240}. Ethylation of any one of these three sites (six per duplex) resulted in strong inhibition of binding (Figure 3B). Overall, the fine structures of the four interference patterns were identical to each other and consistent with the GCN4•CRE structure.[19] This result implies that the relative contribution of each protein•phosphate contact to the overall stability of the peptide•DNA complex is conserved between the metallo-zipper•CRE and disulfide-dimer•CRE complexes, even for contacts to the center of the binding site. In other words, the results of the interference study do not permit us to account for the specificity of the bis(terpyridyl)iron(II) complexes on the basis of dramatic changes in peptide•CRE contacts.

Helical Phasing Analysis. Next we examined whether we could account for the specificity of the bis(terpyridyl)iron(II) complexes on the basis of DNA distortability. The possibility that two DNA sequences might be recognized differentially on the basis of their ability to be deformed was suggested in 1979,[33] and the importance of sequence-dependent deformability for recognition ("indirect readout" [34]) has been confirmed.[35−40] Although GCN4 itself does not bend DNA,[30] other bZIP proteins do.[24,41−44] To determine whether the bis(terpyridyl)iron(II) complexes or the disulfide-dimer peptides distorted DNA when they bound, we made use of a helical phasing assay.[24,43,45] This assay is based on the observation that bent DNA fragments migrate slowly in nondenaturing acrylamide gels when compared to straight DNA fragments and that DNA molecules containing two bends migrate quickly or slowly depending on the relative position and orientation of the two bends.[45] The DNA test fragments we constructed contained a CRE or AP-1 target site separated by a variable length linker from a 25 bp A-tract sequence bent by approximately 54° toward the minor groove (Figure 4A).[24,46] The linker varied the number of base pairs separating the centers of the A-tract and the CRE or AP-1 target site in five steps over one helical turn. A bend induced in the target site upon the binding of a peptide will cause the mobilities of the five peptide•DNA complexes to reach a minimum when the induced and A-tract bends add and to reach a maximum when the induced and A-tract bends negate each other. If no bend is induced in the DNA target site upon peptide binding, then the five test fragments should exhibit the same relative mobility whether they are bound to a peptide or not. Autoradiograms illustrating the primary data are shown in Figure 4B. Note that we did not analyze the AP-1 complexes of the bis(terpyridyl)iron(II) peptides since we could not detect any bound DNA by gel electrophoresis under these conditions.

The helical phasing analysis indicated that the bis(terpyridyl-peptide)iron(II) complexes and the disulfide-dimer peptides induced equivalent bends in the CRE target site and that the bends induced in the AP-1 target site by the disulfide-dimer peptides were identical to those induced in the CRE target site (Figure 4B). To determine the orientations of the induced bends, we plotted the relative mobility of each complex, uncorrected for the mobility of the free DNA, as a function of the distance in base pairs between the center of the A-tract and the center of the test site (Figure 4C). These plots show that, in all six cases, the peptide•DNA complex with the lowest mobility contained 26 bp, or two and one half helical turns of DNA, between the centers of the two sites. Since the lowest mobility complexes resulted when the target site and the A-tract were out of phase, that is, separated by a nonintegral number of helical turns, our analysis indicated that all of the peptides induced major groove bends in the DNA upon binding. A prediction of the estimated bend angles,[43] which are all between 6 and 9 degrees, is shown in Table 2.[47]

The equivalence and the small magnitudes of the induced bend angles support an argument that the CRE/AP-1 target site selectivities of $[G_{28}T_S]_2Fe$ and $[G_{29}T_S]_2Fe$ are not due predominantly to a higher free energy cost for bending the AP-1 target site. The argument is as follows: The CRE complexes of a metallo-peptide and the corresponding disulfide-dimer peptide are virtually identical as judged by their equilibrium dissociation constants (Table 1), sensitivity to phosphate ethylation (Figure 3B), and extent of induced CRE bending in the complex (Figure 4B). Moreover, each disulfide-dimer peptide induces an equivalent bend in the CRE and AP-1 target sites (Table 2) to form disulfide-dimer•CRE and disulfide-dimer•AP-1 complexes of comparable stability (Table 1). Since the AP-1 target site is clearly able to bend by 6−9 degrees to interact with the two disulfide-dimer peptides, there is no obvious reason why it cannot bend by 6−9 degrees to interact with the two metallo-peptides. Although we cannot rule out a differential effect of DNA winding that is hard to detect in our assay, it is unlikely that the low stability of the bis(terpyridyl)iron(II) complex•AP-1

(31) Dervan, P. B. *Science* **1986**, *232*, 464.
(32) Taylor, J. S.; Schultz, P. G.; Dervan, P. B. *Tetrahedron* **1984**, *40*, 457.
(33) Klug, A.; Jack, A.; Viswamitra, M. A.; Kennard, O.; Steitz, T. A. *J. Mol. Biol.* **1979**, *131*, 669.
(34) Otwinowski, Z.; Schevitz, R. W.; Zhang, R.-G.; Lawson, C. L.; Joachimiak, A.; Marmorstein, R. Q.; Luisi, B. F.; Sigler, P. B. *Nature (London)* **1988**, *335*, 321.
(35) Travers, A. A. *Annu. Rev. Biochem.* **1989**, *58*, 427.
(36) Kahn, J. D.; Crothers, D. M. *Proc. Natl. Acad. Sci. U.S.A.* **1992**, *89*, 6343.
(37) Kahn, J. D.; Yun, E.; Crothers, D. M. *Nature (London)* **1993**, *368*, 163.
(38) Walker, S.; Murnick, J.; Kahne, D. *J. Am. Chem. Soc.* **1993**, *115*, 7954.
(39) Sigler, P. B. *Proceedings of the Robert A. Welch Foundation 37th Conference on Chemical Research* **1993**, 63.
(40) Schepartz, A. *Science* **1995**, in press.
(41) Kerppola, T. K.; Curran, T. *Cell* **1991**, *66*, 317.
(42) Kerppola, T. K.; Curran, T. *Science* **1991**, *254*, 1210. Also see: Glover, J. N. M.; Harrison, S. C. *Nature* **1995**, *373*, 257.
(43) Kerppola, T. K.; Curran, T. *Mol. Cell. Biol.* **1993**, *13*, 5479.
(44) Hamm, M. K.; Schepartz, A. *Bio. Med. Chem. Lett.* **1995**, *5*, 1621.
(45) Zinkel, S. S.; Crothers, D. M. *Nature (London)* **1987**, *328*, 178.
(46) Koo, H.-S.; Drak, J.; Rice, A. J.; Crothers, D. M. *Biochemistry* **1990**, *29*, 4227.
(47) It was suggested in 1979 that neutralization of negative charge on one face of a DNA duplex could unbalance repulsive electrostatic interactions between proximal phosphates and cause the DNA to bend toward the neutralized face (Mirzabekov, A. D.; Rich, A. *Proc. Natl. Acad. Sci. U.S.A.* **1979**, *76*, 1118). Indeed, replacement of selected phosphate linkages in a DNA duplex with (uncharged) methylphosphonate analogs causes the DNA to bend toward the neutralized patch (Strauss, J. K.; Maher III, L. J. *Science* **1995**, *266*, 1829). Although it is possible that the +2 charge on each bis(terpyridyl)iron(II) complex leads to the induced bends observed here, we view this possibility to be unlikely because the two disulfide-dimer peptides (which lack this +2 charge) also bend DNA.

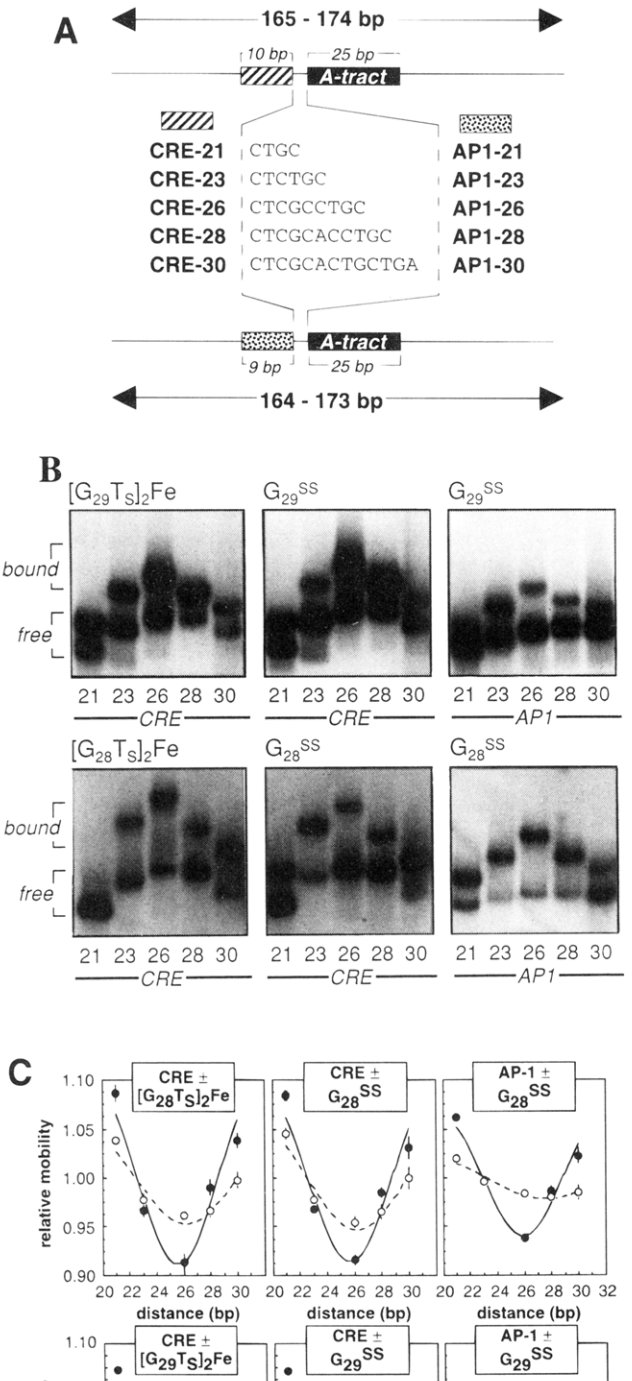

Figure 4. Phasing analysis of the DNA complexes of metallo- and disulfide-dimer peptides. (A) Probes used for phasing analysis contained a CRE (striped box) or AP-1 (dotted box) target site separated by a variable length linker from a 25 bp A-tract sequence.[24] Probes are named (ex: CRE-26) by the sequence of DNA within the test site (CRE or AP-1) followed by the number of base pairs separating the center of the CRE (or AP-1) target site and the center of the A-tract. With the exception of the variable linker, all probes were the same size and contained the same sequence.[24] (B) Electrophoretic mobility shift analysis of peptides bound to phasing analysis probes. (C) Relative mobilities of the free (○) and bound (●) DNAs were calculated as described[24] and represent the average of at least eight independent experiments. Error bars represent the standard deviation. The points are connected by the calculated best fit of the data to a cosine function.[43]

Table 2. Estimated Bend Angles of the CRE and AP-1 Target Sites in the Presence and Absence of the bZIP Peptide Models G_{28}^{SS}, G_{29}^{SS}, $[G_{28}T_S]_2Fe$, and $[G_{29}T_S]_2Fe$ at 4 °C[c]

peptide	CRE,[a] deg	AP-1, deg
none	11 ± 1[b]	4 ± 1
G_{28}^{SS}	19 ± 3	13 ± 2
G_{29}^{SS}	17 ± 2	12 ± 1
$[G_{28}T_S]^2Fe$	20 ± 3	N.D.
$[G_{29}T_S]_2Fe$	17 ± 2	N.D.

[a] Reactions were performed and analyzed as described in the Experimental Section. [b] Values represent the average of at least eight experiments. Error bars represent the standard deviation. [c] All values represent bends toward the major groove.

complexes results from a high free energy cost for bending the AP-1 target site. Note in addition, the average free energy required to bend DNA smoothly in an elastic model by 9° over 10-bp is <0.1 kcal mol^{-1} and therefore cannot easily account for the 2−4 kcal·mol^{-1} lower stability of the metallopeptide·AP-1 complexes.[48]

G_{28}-bipy-G_{28}. Despite the similarities in the recognition interfaces of the CRE and AP-1 target sites, these two sequences still differ by a base pair in the center, and it is here where they should differ most in structure (even with the intrinsic CRE bend). This difference in structure is, apparently, invisible to G_{29}^{SS} and G_{28}^{SS}, but not to $[G_{29}T_S]^2Fe$ and $[G_{28}T_S]_2Fe$. Given that G_{28}^{SS} and $[G_{S8}T_S]_2Fe$ differ most in terms of the structural demands of their dimerization domains, we considered the possibility that the specificity exhibited by the two bis(terpyridyl)iron(II) complexes resulted from the inability of the AP-1 target site to accommodate the bulk of the bis(terpyridyl)iron(II) complex. This explanation would be consistent with our earlier experiments which indicated that the CRE-specificities of bis(terpyridyl-peptide)iron(II) complexes resulted from destabilizing interactions with the AP-1 sequence.[15]

To test this hypothesis we synthesized G_{28}-bipy-G_{28} (Figure 5A). This molecule contained two copies of the peptide found in $[G_{28}T_S]_2Fe$ linked by a 5,5′-disubstituted bipyridyl moiety in place of the bis(terpyridyl)iron(II) complex. This bipyridyl spacer mimics the bis(terpyridyl)iron(II) complex in terms of the distance between the two benzylic carbons (10.0 Å versus 12.3 Å, respectively), and peptides attached to the two linkers possess equivalent conformational flexibilities. The bipyridyl spacer is, however, considerably less demanding sterically than is the bis(terpyridyl)iron(II) complex; the former fits into a cylinder 10 Å in length and 4 Å in diameter, whereas the latter fits into a sphere of 12 Å diameter. The affinity of G_{28}-bipy-G_{28} for the CRE and AP-1 target sites was measured by direct gel mobility shift analysis. Plots showing the relative affinity of G_{28}-bipy-G_{28} for the CRE and AP-1 target sites are shown in Figure 5B; data for $[G_{28}T_S]_2Fe$ are shown for comparison. Equilibrium dissociation constants are listed. Under these conditions, G_{28}-bipy-G_{28} showed a 0.9 kcal·mol^{-1} preference for the CRE target site, behaving much like G_{28}^{SS} (see Table 1). $[G_{28}T_S]_2Fe$, which displayed a 1.9 kcal·mol^{-1} preference for the CRE target site under these conditions, was decidedly more selective. Note that under these higher salt conditions we can detect the $[G_{28}T_S]_2Fe$·AP-1 complex.

Discussion

The experiments described here were initiated to understand how the bis(terpyridyl)iron(II) complexes shown in Figure 1 modify the inherent selectivity of the GCN4 DNA recognition peptide without altering its sequence. These molecules contain all of the information necessary to recognize the CRE and AP-1

(48) Liu-Johnson, H.-N.; Gartenberg, M. R.; Crothers, D. M. *Cell* **1986**, *47*, 995.

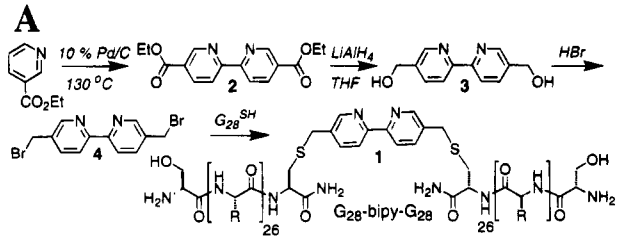

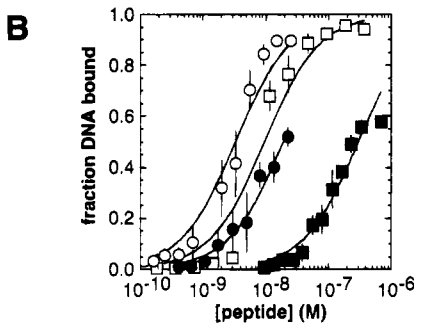

K_d (ΔG^o_{obs})

	CRE	AP-1
G_{28}-bipy-G_{28}	3.4 ± 0.4 nM (-10.7)	19.6 ± 1.3 nM (-9.8)
$[G_{28}T_S]_2Fe$	9.6 ± 1.8 nM (-10.2)	300 ± 26 nM (-8.3)

Figure 5. (A) Scheme illustrating the synthesis of G_{28}-bipy-G_{28}. (B) Semilogarithmic plots illustrating the fraction of ^{32}P CRE_{24} (open symbols) or ^{32}P AP-1_{23} (shaded symbols) bound to G_{28}-bipy-G_{28} (circles) or $[G_{28}T_S]_2Fe$ (squares) as a function of the total peptide concentration. Solid lines represent the best fit of the data to eq 1.

target sites, as judged by the X-ray crystal structures of the GCN4•CRE and GCN4•AP-1 complexes.[18,19] Yet, unlike GCN4, and unlike disulfide-dimer peptides derived from GCN4,[14,15,25,26] the bis(terpyridyl)iron(II) complexes discriminate between the CRE and AP-1 target sites. The magnitudes of the CRE/AP-1 specificities exhibited by $[G_{29}T_S]_2Fe$ and $[G_{28}T_S]_2Fe$ are comparable to those exhibited by natural bZIP proteins such as CRE-BP1 and ATF-2.[22,44] When we first began these experiments there was no indication that either the CRE or the AP-1 target site populated anything other than a standard, B form conformation. On this basis, it seemed likely that the selectivities of the metallo-zipper peptides resulted from the inability of the rigid bis(terpyridyl)iron(II) complex to "contract" to position the G_{29} or G_{28} peptides into a conformation suitable for binding the more compact AP-1 target site. The discovery that the CRE target site bends intrinsically toward the major groove and resembles the AP-1 target site required a reevaluation of this explanation.[24]

Our initial experiments indicated that the bis(terpyridyl)iron-(II) complexes interacted with the CRE target site in a manner that was indistinguishable from that of the disulfide-dimer peptides. Quantitative competition experiments showed that the stabilities of the two bis(terpyridyl)iron(II) complex•CRE complexes paralleled those of the corresponding disulfide-dimer•CRE complexes. Even the stabilities of the nonspecific DNA•bis-(terpyridyl)iron(II) complexes paralleled those of the corresponding nonspecific DNA•disulfide-dimer complexes. In addition, the phosphate interference patterns of the two bis-(terpyridyl)iron(II) complex•CRE complexes superposed on those of the corresponding disulfide-dimer•CRE patterns. The similarity of the four interference patterns suggested that all four peptides interacted with the CRE target site in much the same way. Although the presence of the terpyridyl complex dramatically lowers the affinity of the metallo-peptide for the AP-1 target site, there is no evidence that it affects interactions of the peptide with the CRE target site.

The observation that specificity is eliminated when the bis-(terpyridyl)iron(II) complex is replaced with a sterically less demanding bipyridyl moiety strongly implicates the bulk of the metal complex as the underlying physical basis for sequence specificity. However, it is unlikely that the metal complex interacts directly with the DNA; the structures of the GCN4•CRE and GCN4•AP-1 complexes suggest that the edge of the metal complex is more than 12 Å from the phosphodiester backbone of the AP-1 target site.[18,19] It is more likely that the bis-(terpyridyl)iron(II) complex exerts its effect on the conformation of the proximal region of the peptide, a region known as the spacer segment. It is notable in this regard that the spacer segment residue Arg_{249} (the only residue within the spacer segment that contacts DNA directly) participates in different contacts in the CRE and AP-1 complexes of GCN4.[18,19] In the GCN4•AP-1 complex, the Arg_{249} side chain contacts an unesterified oxygen of the $A_{-4}pT_{-3}$ phosphate (see Figure 1 for numbering scheme). In the GCN4•CRE complex, the Arg_{249} side chain participates in an intramolecular ionic interaction with Glu_{254}, which is located within the zipper segment. In this case, the $A_{-4}pT_{-3}$ phosphate (numbered $A_{-5}pT_{-4}$ in ref 19) is recognized by the side chains of Arg_{245} and Arg_{241}. Interference experiments have shown the $A_{-4}pT_{-3}$ phosphate in the GCN4•AP-1 complex to be extremely sensitive to phosphate ethylation.[30] Although it is unlikely that the specificity of $[G_{29}T_S]_2Fe$ and $[G_{28}T_S]_2Fe$ results entirely from the absence of a single protein•DNA contact (Figure 3B), small changes in conformation within the spacer segment that are propagated down the helix could misalign a number of contacts; the net result would be a very large change in binding affinity. Indeed, there is considerable evidence that the high CRE/AP-1 specificities exhibited by certain CREB/ATF bZIP proteins (such as CRE-BP1 and CREB) are controlled, at least in part, by a few residues within the spacer segment that do not contact DNA.[22,49] Replacement of three residues in the GCN4 spacer segment (L_{247}, R_{249}, M_{250}) with the corresponding residues of CREB (K_{304}, Y_{306}, and V_{307}) generates a peptide that binds preferentially by a factor of 2 to the CRE target site;[49] replacement of the entire GCN4 spacer segment with the corresponding residues of CRE-BP1 generates a peptide that binds preferentially by a factor of 4 to the CRE target site. Thus, it is possible that the non-natural bis(terpyridyl)iron(II) complexes and the natural CRE-selective bZIP proteins CREB and CRE-BP1 may employ a common mechanism for avoiding an interaction with the AP-1 target site. In conclusion, the observation that subtle and indirect effects on the conformation of a small peptide can lead to large changes in CRE/AP-1 specificity provides further evidence that it may be possible to design surprisingly small molecules that bind DNA with high sequence-specificity as well as high affinity.

Experimental Section

Peptides. $[G_{28}T_S]_2Fe$ and G_{28}^{SS} were synthesized as described previously.[14,15,20] The synthesis of G_{28}-bipy-G_{28} is described below. All peptides were characterized by mass spectroscopy, amino acid analysis, and UV/visible spectroscopy. NMR spectra were recorded on a Brucker WM 250 spectrometer. Chemical shifts are reported in ppm downfield from $(CH_3)_4Si$, and coupling constants are given in Hertz. IR spectra were recorded on a Perkin Elmer 1600 FT-IR spectrometer. Mass spectra were recorded on a Hewlett-Packard 5988 spectrometer equipped with an electrospray source. AAA was performed in triplicate using a Beckman 73000 analyzer with norleucine and homoserine as internal standards. Cysteine was not determined. UV/visible spectra were recorded on a Perkin-Elmer Lambda 6 instrument. Samples were dissolved in 10 mM potassium phosphate

(49) Kim, J.; Tzamarias, D.; Ellenberger, T.; Struhl, K.; Harrison, S. C. *Proc. Natl. Acad. Sci. U.S.A.* **1993**, *90*, 4513.

buffer (pH 7.4). λ_{max} and ϵ are reported in units of nanometers and $10^4 \cdot cm^{-1} \cdot M^{-1}$, respectively. Data: $\mathbf{G_{28}T_S}$: MS calculated for $C_{149}H_{253}N_{59}O_{37}S_3$: 3559.2; found: 3561.1. AAA expected, $Asx_2Thr_1Ser_1Glx_3Ala_6Met_1Leu_2Lys_3Arg_7$; found, $Asx_{2.1}Thr_{0.9}Ser_{0.9}Glx_{3.1}Ala_{6.1}Met_{1.0}Leu_{2.0}Lys_{3.1}Arg_{6.3}$. $\mathbf{[G_{28}T_S]_2Fe}$: MS calculated for $C_{298}H_{506}N_{118}O_{74}S_6Fe_1$: 7174.3; found: 7174.1. AAA expected, $Asx_4Thr_2Ser_2Glx_6Ala_{12}Met_2Leu_4Lys_6Arg_{14}$; found, $Asx_{4.3}Thr_{1.9}Ser_{1.8}Glx_{6.3}Ala_{12.6}Met_{1.9}Leu_{4.1}Lys_{6.3}Arg_{13.1}$. UV/vis λ_{max} (ϵ) 280 (5.3), 321 (4.7), 561 (1.6). $\mathbf{G_{28}^{SS}}$: MS calculated for $C_{266}H_{482}N_{112}O_{74}S_4$: 6561.7; found: 6562.7. AAA expected, $Asx_4Thr_2Ser_2Glx_6Ala_{12}Met_2Leu_4Lys_6Arg_{14}$; found, $Asx_{4.3}Thr_{1.9}Ser_{1.9}Glx_{6.4}Ala_{12.5}Met_{1.8}Leu_{4.2}Lys_{6.3}Arg_{13.1}$.

5,5'-Dihydroxymethyl-2,2'-bipyridine (3). To a solution of 5,5'-dicarbethoxy-2,2'-bipyridine (**2**), prepared according to the method of Rotzinger[50] (2 g, 6.67 mmol) in THF (250 mL) at 25 °C was added 1 M $LiAlH_4$ in THF (20 mL) over a period of 60 min. The orange reaction mixture was stirred at 25 °C until it turned pale yellow. Anhydrous sodium sulfate (~2 g) was added, and the mixture was filtered. The filtrate was evaporated to dryness, and the residue was chromatographed on silica gel (15:85 MeOH:CH_2Cl_2) to afford 631.3 mg (44%) of diol (**3**) as a pale yellow solid: ^1H NMR (MeOH-d_4) δ 8.55 (d, J = 2 Hz, 2H, H6), 8.2 (d, J = 8 Hz, 2H, H3), 7.85 (dd, J = 8, 2 Hz, 2H, H4), 4.64 (s, 4H, CH_2); mp 155−159 °C (lit. 157−161 °C).[51]

5,5'-Bis(bromomethyl)-2,2'-bipyridine (4). 5,5'-Dihydroxymethyl-2,2'-bipyridine (**3**) (22 mg, 101.8 mmol) was heated to reflux in 47−49% HBr (5 mL) for 4 h. The reaction was cooled to room temperature, and 5 mL aliquots of H_2O and CH_2Cl_2 were added. The aqueous layer was neutralized to pH ~ 8 with 10% Na_2CO_3 and extracted three times with CH_2Cl_2. The combined organic extracts were concentrated under reduced pressure, and the residue was chromatographed on silica gel (2% MeOH in CH_2Cl_2) to yield 10.2 mg (29%) of the dibromide as a fine white powder: ^1H NMR ($CDCl_3$) δ 8.66 (d, 2H, J = 2.1 Hz, H6), 8.4 (d, 2H, J = 8.3 Hz, H3), 7.8 (dd, 2H, J = 8.2, 2.3 Hz, H4), 4.52 (s, 4H, CH_2); ^{13}C NMR ($CDCl_3$) δ 29.75 (CH_2), 120.65, 137.8, 149.5 (CH), 134.2, 153 (C); FT-IR ($CHCl_3$) 3500, 3280, 2395, 2360; mp 199−200 °C (lit. 211 °C);[52] mass spec (FAB, PNDBA matrix) calculated for $C_{12}H_{10}N_2Br_2$ [M + H] 340.9289, found 340.9288.

G_{28}-bipy-G_{28} (1). All solutions were deoxygenated before use. To 45 μL of a 1 mM CH_3CN solution of 5,5'-bis(bromomethyl)-2,2'-bipyridine (**4**) was added 100 μL of a 1 mM solution of G_{28}^{SH} in 100 mM phosphate buffer (pH 8.0). An additional 55 μL of CH_3CN was added, and the reaction was incubated at 25 °C for 6 h. Ten microliters of 1 M DTT was added, and the reaction products were separated and purified by reverse phase HPLC (column: Vydak Protein/Peptide C_{18} 300 Å; linear gradient of 9.8%−72.2% CH_3CN with 0.1% TFA over 30 min). Retention times were as follows: G_{28}^{SH}, 14.7 min; G_{28}^{SS}, 15.7 min; G_{28}-bipyridine-G_{28}, 16.1 min. G_{28}-bipyridine-G_{28} was differentiated from G_{28}^{SH} on the basis of its unique absorbance at 280 nm. The product was recovered in an 11% yield as measured by UV. Amino acid analysis expected: $Asx_4Thr_2Ser_2Glx_6Pro_2Ala_{12}Met_2Leu_4Lys_6Arg_{14}$; found, $Asx_{4.4}Thr_{2.0}Ser_{2.0}Glx_{6.7}Pro_{2.2}Ala_{12.3}Met_{2.1}Leu_{4.4}Lys_{6.3}Arg_{14.0}$; mass spec (electrospray; 50% 2-propanol, 0.1% formic acid) calculated for $[M^+]$ 6746, found 6744.

Electrophoretic Mobility Shift Analysis. Binding reactions in Figure 2A were performed by incubating the indicated peptide at 4 °C with <50 pM of 5' end-labeled CRE_{24} or AP-1_{23} in binding buffer (10 mM potassium phosphate pH 7.4, 100 mM KCl, 0.1% Nonidet P-40, 5% glycerol). These conditions correspond exactly to those used in the competition analysis (Table 1). Binding reactions in Figure 5B were performed by incubating the indicated peptide at 4 °C with <50 pM of 5' end-labeled CRE_{24} or AP-1_{23} in PBS binding buffer (10 mM Na_2HPO_4, 2 mM KH_2PO_4 (pH 7.4), 138 mM NaCl, 2.7 mM KCl, 10 mM EDTA, 1 mM DTT, 5% glycerol, 0.1% NP-40, 40 μg/mL BSA). After a 30 min incubation, the reactions were loaded directly on a nondenaturing 10% (49:1 acrylamide:bis-acrylamide) (Figure 2A) or 8% (32:1 acrylamide:bis-acrylamide) (Figure 5B) polyacrylamide gel prepared in running buffer (20 mM Tris base and 153 mM glycine (pH 8.9 at 4 °C)). Gels were maintained at 4−6 °C during electrophoresis by immersion in running buffer cooled by a circulating, temperature-controlled water bath. The amounts of complexed and free DNA were quantified using a Betagen 603 Blot Analyzer (Betagen Co.). Dissociation constants were determined by fitting the data to the Langmuir equation

$$\Theta = \frac{1}{1 + \frac{K_{app}}{[\text{peptide}]_T}} \quad (1)$$

with K_{app} as the adjustable parameter and Θ = fraction DNA bound = cpm bound DNA/(cpm bound DNA + cpm free DNA) using a nonlinear least squares fitting program (KaleidaGraph 2.1.2, Abelbeck Software). Values represent the average of at least three independent experiments ± the relative standard error of estimate $S_y = 100[S(F_T - F_E)^2/n]^{1/2}/\langle F_E \rangle$. F_T and F_E are the fractions bound as determined from theory and experiment, respectively, and n is the number of data points.[53]

Competition Experiments. These experiments were performed as described previously.[15] Briefly, to a mixture of unlabeled DNA (55 pM−40 μM) and < 7.5 pM 5' end-labeled CRE_{24} in binding buffer was added 4 nM peptide in binding buffer (final volume 10 μL). Solutions were incubated for 1 h at 4 °C before being applied to a running native gel as described.[15] Oligonucleotide sequences: CRE_{24}, AGTGGAGATGACGTCATCTCGTGC; AP-1_{23}, AGTGGAGATGACTCATCTCGTGC; C30, GATATCCCTGTTACGACTTGAGGATCAAAG; SCR, AGTGGAGTAAGGCCTATCTCGTGC. Dissociation constants were determined by fitting the data to equation

$$\Theta = \frac{\left(K_{PC} + \frac{K_{PC}}{K_{PA}} + P_T + C_T - \sqrt{\left(K_{PC} + \frac{K_{PC}}{K_{PA}}A_T + P_T + C_T\right)^2 - 4C_TP_T}\right)}{2C_T} \quad (2)$$

where P_T, A_T, and C_T are, respectively, the total concentration of peptide, competitor DNA, and radiolabeled CRE_{24}. PC represents the concentration of radiolabeled CRE_{24}:peptide complex and PA represents the concentration of peptide·competitor complex. K_{PC} represents the dissociation constant for peptide binding to CRE_{24}, and K_{PA} represents the dissociation constant for peptide binding to competitor. Error bars represent the standard deviation of at least three experiments.

Interference Assays. Sixty-five bp oligonucleotides containing a central CRE target site (CRE_{65}^+ top (+) strand) or its complement (CRE_{65}^- bottom (−) strand) were prepared by solid-phase synthesis. Ten picomoles of each strand were 5' end labeled with T4 polynucleotide kinase (New England Biolabs) and [γ-^{32}P] ATP (17 pmoles, Dupont) in a total volume of 20 μL. The reaction products were extracted with phenol and chloroform, and the DNAs were precipitated, washed with ethanol, and dried. The pellets were dissolved in 20 μL of annealing buffer (10 mM Tris·Cl, 100 mM KCl (pH 7.4)), heated to 90 °C, cooled slowly to room temperature, ethanol precipitated and washed, and dissolved in water to provide the CRE_{65} duplex. Generation of phosphate-modified DNA: 3 pmol 5' end labeled CRE_{65} was suspended in 100 μL of a solution containing 50 mM sodium cacodylate and 1 mM EDTA (pH 8). Six microliters salmon sperm DNA (1 mg/mL) were added, and the solution was cooled to 0 °C. One hundred microliters of an ethylnitrosourea-saturated ethanol solution was added, and the reactions were incubated for 1 h at 50 °C. The reaction mixture was cooled to 0 °C, and the DNA precipitated by the addition of 20 μL of 3 M sodium acetate, 20 μL of $MgCl_2$, 10 μL of transfer RNA (1 mg/mL, Sigma), 40 μL of water, and 400 μL of absolute ethanol. The pellet was rinsed with 70% ethanol, dried, and dissolved in water. The final volume of water was adjusted so that the solution radioactivity was 2 × 10^5 cpm/μL. Separation of bound and free modified DNAs: Modified CRE_{65} (2 × 10^6 cpm) was incubated with peptide (100 nM) for 30 min at 4 °C in binding buffer containing 10 μg/mL bovine serum albumin. Free and peptide-bound CRE_{65} were separated by nondenaturing polyacrylamide gel electrophoresis (8%, 80:1 acrylamide:bis-acrylamide) using 10 mM Tris·Cl (pH 7.4), 1.0 mM EDTA at 4 °C. Dissociation constants of the modified CRE_{65}·peptide complexes ranged

(50) Rotzinger, F. P.; Munavalli, S.; Comte, P.; Hurst, J. K.; Gratzel, M.; Pern, F.; Frank, A. J. *J. Am. Chem. Soc.* **1987**, *109*, 6619.
(51) Whittle, C. P. *J. Heter. Chem.* **1977**, *14*, 191.
(52) Ebmeyer, F.; Vogtle, F. *Chem. Ber.* **1989**, *122*, 1725.
(53) Devore, J. L. *Probability and Statistics for Engineering and the Sciences*; Brooks/Cole: Monterey, 1987.

from 50 to 100 nM. Free and bound CRE_{65} were visualized by autoradiography and eluted by use of an Elutrap (Schleicher & Schvell) in 40 mM Tris-borate (pH 8.0). The eluted samples were lyophilized and desalted by ethanol precipitation. Cleavage of modified CRE_{65}: recovered free and bound CRE_{65} pools were dissolved separately in 30 μL of AE buffer (30 mM sodium acetate, 0.01 mM EDTA (pH 8.0)). Seven microliters of 1 M NaOH were added, and the mixture was incubated at 90 °C for 30 min. Seven microliters of 1 M HCl were added, the mixture was cooled to 4 °C, and the DNA was ethanol precipitated. The pellets were suspended in 98% (v/v) formamide, 0.05% bromophenol blue and xylene cyanol, heated for 1 min to 100 °C, and chilled on ice, and equivalent amounts of radioactivity for both the bound and free fractions were loaded on a 20% (10:1 acrylamide: bis-acrylamide) sequencing gel. The resulting gel were analyzed by autoradiography, and the radioactivity was quantified for each band using a Betascope 603 Blot Analyzer (Betagen).

Phasing Analysis. The indicated peptide (0.5−1.5 nM) was added to 10−100 pM end-labeled, double stranded DNA (5000−20 000 cpm) and incubated for 30 min at 4 °C in a final reaction mixture (10 μL) containing 10 mM Tris•Cl pH 7.4, 100 mM KCl, 5% glycerol, 0.1% NP-40, and 1 μg BSA. Free and peptide-bound DNA were resolved by nondenaturing 8% (32:1) polyacrylamide gel electrophoresis in 0.5X TG buffer (12.5 mM Tris, 108 mM glycine pH 8.9) at 4 °C and 12 $V \cdot cm^{-1}$. Radioactivity was quantified using a Betascope 603 Blot Analyzer (Betagen).

Acknowledgment. This work was supported by the N.I.H. and the National Foundation for Cancer Research. A.S. is a David and Lucile Packard Fellow, an NSF Presidential Young Investigator, a Camille and Henry Dreyfus Teacher-Scholar, an Alfred P. Sloan Foundation Research Fellow, and a 1995 Arthur C. Cope Scholar. C.R.P. and L.S.S. were supported by N.S.F. predoctoral fellowships, J.C.A. was supported by an N.I.H. postdoctoral fellowship, B.C. was supported by an Arthur Wayland Dox fellowship, and D.N.P. was supported by an N.I.H. Training Grant in Biophysics. We are grateful to the Keck Foundation Biotechnology Resource Laboratory at Yale for peptide and oligonucleotide synthesis.

JA951192E